TECHNICAL MEMORANDUMS

NATIONAL ADVISORY COMMITTEE FOR AERONAUTICS

No. 722

GUIDE VANES FOR DEFLECTING FLUID CURRENTS WITH SMALL LOSS OF ENERGY

By G. Kröber

Ingenieur-Archiv, Vol. III, 1932

Washington
September 1933

NATIONAL ADVISORY COMMITTEE FOR AERONAUTICS

TECHNICAL MEMORANDUM NO. 722

GUIDE VANES FOR DEFLECTING FLUID CURRENTS WITH SMALL LOSS OF ENERGY*

By G. Kröber

I. INTRODUCTION

Numerous articles have already been written regarding currents in bent pipes and elbows and on the present problem, namely improving the flow in a sharp bend by installing guiding devices. Nevertheless the designing of wind tunnels for aerodynamic experiments called for new and more comprehensive tests. There was also need of improving the flow in the bends of gas and liquid conduits, as, e.g., in the smoke flues and ventilating shafts of large factories.

Several devices have been tested in wind tunnels (reference 1), and the results of a series of model tests in bends (reference 2) and elbows (reference 3) with built-in partitions and guide vanes have already been published. There is, however, some hesitation about adopting these forms for newly projected wind tunnels, in which the maximum economy in the driving force is necessary, due to the much greater performances required. Since the previous forms were determined empirically for the most part, there was no way of telling whether they could be used in other dimensions without modification. In particular the influence of the cross-sectional shape of the tunnel was not fully determined.

Every deflection of a liquid or gas current involves losses and a disturbance of the state of motion. When there is a regular velocity profile more or less developed before the deflection according to the length of the approach (reference 4), an entirely different picture is observed after the deflection (reference 5). A new velocity distribution is produced by the centrifugal forces. There

---

*"Schaufelgitter zur Umlenkung von Flüssigkeitsströmungen mit geringem Energieverlust." Ingenieur-Archiv, vol. III, 1932, pp. 516-541.

are also disturbances due to friction (secondary flows and separation from the outer and inner walls). The energy losses and the disturbance of the velocity distribution in flowing through a bend or elbow increase with the sharpness of the bend. The energy losses may amount to about 100 percent of the momentum of the flowing medium, as based on the mean velocity in the inlet cross section* (reference 6).

The main reason for the great losses in the standard bends with small radius of curvature is the marked separation from the inner side of the bend. To this are added the losses due to the lost kinetic energy of the vortices of the secondary flow and to the increased friction in the adjoining channel resulting from uneven velocity distribution and from the consumption of energy in the restoration of the undisturbed distribution.

It is therefore of prime importance to adopt measures for preventing separation and secondary flows. The most effective remedy is the division of the curved portion of a broad channel with unfavorable ratio of the radius of curvature R to the width b into a series of narrower channels with more favorable R/b ratio.

The transverse momentum of the deflected air stream to be absorbed is divided between all the intermediate and outside walls, so that the pressure increase on each wall is much smaller and the danger of separation is diminished. The formation of secondary vortices is also greatly diminished.**

There are two principal ways of dividing the channel:

1. Division of a bend with unfavorable R/b ratio by installing partitions throughout the entire bend, as shown in figure 1, the widths of the individual channels being so adjusted that each will have the same R/b ratio.

---

*The writer obtained about 160 percent in an elbow of square cross section and very short approach.

**Aside from the possibility of improvement by the installation of partitions, there are also other ways for attaining the same goal. I have in mind particularly the removal of the boundary layer by suction, although this method has yet yielded no positive results. Since this method, moreover, necessitates great expenditures for structural parts, wind tunnels, and sometimes even pumps, etc., it is seldom employed.

2. The installation of wing-like guide vanes which produce the requisite transverse force for deflecting the air stream. These vanes may be either plain (fig. 2a) or streamlined (fig. 2b).

The first way (fig. 1) was once quite thoroughly investigated by the writer. In order to obtain a good velocity distribution in the cross section immediately after the bend, it was necessary to install a large number of partitions. This naturally entailed much surface friction, which was manifested in a high resistance and great reduction of the velocity behind the partitions. In the most favorable case the energy loss was 23 to 24 percent of the original momentum, while losses of only about 15 percent with wing-like guide vanes had been obtained in previous years.

In experiments with partitions in the bend, it was found best to widen all the component channels in the middle of the bend in such a way as gradually to diminish the curvature of the walls from the leading edge to the trailing edge.*

When it is desired to deflect a current so that its nature (i.e., its velocity and pressure distributions throughout the cross section) will be disturbed as little as possible, the deflection is best produced by only one set of vanes forming a sort of "grid" without involving the walls, since otherwise, due to their fundamentally different shape with respect to the air stream (the outer wall being concave and the inner wall convex), unsymmetrical relations always exist. The problem is therefore to develop a form of grid, which will deflect a current through a large angle with good efficiency without affecting its velocity.

It seems logical, in calculating the guide vanes, to assume a pure potential flow. Closer investigation, however, shows that this alone does not suffice. Rather it is necessary to allow for the effect of the energy loss on the pressure distribution over the guide-vane profiles. This is done in what follows. The effect of the viscosity on the loss of energy is also considered, and, lastly, the results of an investigation of the vortex region behind the

---

*The subsequently reported Nippert experiments showed that it was advisable to reduce the radius of the outside wall of a right-angle bend so that the channel would be somewhat wider in the center of the bend.

guide vanes are given.

There is a fundamental difference between the present investigation and the previously reported investigations by Christiani (reference 6), Schilhansl (reference 7) and others (reference 8). The object of these investigations was to determine the physical flow characteristics of given profile forms, while here a method is shown for determining a profile form with definite characteristics (definite circulation).

II. DETERMINATION OF FAVORABLE PROFILE FORMS IN CURVILINEAR CURRENTS*

1. The Method

The method proposed here for the development of the guide vanes is based on the following line of reasoning. The flow through the deflecting grid may be regarded in first approximation as a potential flow. According to the method of Dr. Betz (references 9 and 10) we will first imagine the guide vanes replaced by a series of concentrated vortices. The strength of each vortex must equal the circulation about the vane replaced by it and is easily calculated from the required deflection of the flow for a predetermined distance between the vanes.

In the field of potential flow determined by the vortex strength and the inflow velocity, a profile, whose characteristics in parallel planar flow are known and which has the requisite circulation, is conformally transformed, so that the center of gravity of its circulation falls in the line connecting the individual vortices replacing the other vanes. In the transformation we must allow for the effect of friction, as already indicated. In the transformation of the profile, the curvature is changed and consequently the pressure distribution, as likewise the pressure increase which in turn produces significant changes in the behavior of the boundary layers. In this work it was found that the displacement of the center of gravity of the circulation may considerably affect the results.

---

*In the preparation of this section, I have been greatly assisted by Dr. Betz.

From the outset we must expect that the deflecting system, thus determined, will always require certain corrections, since the field of flow, which forms the basis for the transformation, can be only approximately correct. A second approximation can be made, not by calculating the field of flow with the aid of concentrated vortices, but by suitably distributing the circulation over the profile found according to the first approximation and then calculating anew the field of flow and repeating the transformation. (This "detachment" of the vortex is possible only when the first approximation of the profile form is known, since there is otherwise no basis for the location of the elementary circulation).

2. Development of the Profile of First Approximation

a) Calculating the field of flow.- We will first consider a flow deflection of 90 degrees. The potential function of the vortex series, which is conceived as replacing the vane can be calculated, since the plane of the grid (which will be called the z plane) can be represented by a simple periodic function on a plane with only a single vortex (ζ plane) (reference 9).

A graphic method based on this relationship, as proposed by Betz (reference 10), was used for plotting the flow diagram. The flow through the grid can be represented by the superposition (1) of a parallel flow perpendicular to the direction of the grid and (2) of a flow which is produced by all the vortices replacing the vanes and which is essentially parallel to the grid and therefore causes the deflection of the current (fig. 3).

In figures 3 and 4 we have: s, division of grid (= distance between vortices); v, velocity component normal to direction of grid; u, velocity component parallel to grid; w, resultant velocity before and behind grid.

At a great distance from the grid (fig. 3):

1. The velocity components $v_1 = v_2$, resulting from the parallel flow. (At a great distance, the vortex series produces no motion normal to the grid direction).

2. The velocity components u_1 and u_2, resulting from the vortex series $u_2 = -u_1$.

Near the grid we must distinguish (fig. 4) between $V = v + v'$ and $U = u'$, where v' and u' are the flow velocities induced by the vortex series. (In unsymmetrical flow involving a change of w another parallel component u had to be added.)

In figure 3, if a field of the width s is laid out the line integral along the boundary lines is just equal to the circulation of a vortex. The length l is so great that, in the field of the boundary lines parallel to the grid, the fluctuations of U and V have died out. The circulation then becomes

$$\Gamma = s\,u_1 + \int_{-l/2}^{+l/2} V\,dl - s\,u_2 + \int_{+l/2}^{-l/2} V\,dl$$

or

$$\Gamma = s(u_1 - u_2)$$

since

$$\int_{-l/2}^{+l/2} V\,dl = -\int_{+l/2}^{-l/2} V\,dl$$

The total deflection, corresponding to the problem, is 90 degrees, and w therefore incloses, with u, an angle of 45 degrees. Hence we can also write

$$\Gamma = s\,w\sqrt{2}$$

Now the velocity components u' and v' resulting from the vortex series can be calculated in a simple way with the aid of the Betz graphs at sufficient points of the field. The flow diagram can be plotted after the addition of the velocity components v.

In order to decide how the profile must be introduced into the flow, one must know how the field of flow appears when the vortex is absent at the point where the vane is to stand. One desires to remove the vane from the simple parallel flow, i.e., by conformal transformation and appropriately utilizes for this purpose the streamline diagram as it appears when the vane is not present (straight streamlines and straight potential lines perpendicular to them). The other vortices are necessary, since the curved field is only created by them as a whole (being always infinitely many, notwithstanding the missing one). The Betz graphs

are also used for the case when a vortex is missing. Figure 5 is the flow diagram of the series with one vortex missing.

b) Determining the dimensions of the basic profile (single vane is rectilinear flow) and transfer to the curved field.- A single vane in a rectilinear flow is subjected to a "lift" of

$$A = \rho w_e \Gamma_e = c_a \frac{\rho}{2} w_e^2 t$$

in which we have:

w_e, velocity of parallel flow in infinity (m/sec);
t, chord of vane (m);
c_a, lift coefficient;
ρ, density of flowing medium (kg sec^2/m^4).

The circulation about each vane is therefore

$$\Gamma_e = \frac{1}{2} c_a w_e t \qquad (1)$$

On the other hand, the circulation about the guide vane is

$$\Gamma_g = s w_g \sqrt{2} \qquad (2)$$

when w_g is the resultant velocity for before and behind the grid. Since, in conformal transformation, the circulation is maintained, we have

$$\Gamma_e = \Gamma_g$$

or

$$\frac{1}{2} c_a w_e t = s w_g \sqrt{2} \qquad (3)$$

according to equations (1) and (2). The scale for the coordinates of the z and ζ planes are so chosen that $w_e = w_g = w$. We thus obtain the same coordinate systems in both planes at a great distance from the profile. Applying this to equation (3), we obtain

$$t = \frac{2\sqrt{2}}{c_a} s \qquad (4)$$

According to figure 6, in which

$$s = \frac{b\sqrt{2}}{n}$$

(b = width of square channel, for which the grid series is calculated, measured normal to w; n = number of vanes, the inner and outer wall counting together as one vane), we have

$$t = \frac{4\ b}{n\ c_a} \tag{5}$$

In order to obtain vanes with chords corresponding somewhat to tested forms, we admit $c_a = 1.35$. Then we do not need to fear that the lift-drag ratio will be unfavorable. The correctness of this assumption is confirmed by tests, especially by photographs of the flow*.

We will choose a profile form corresponding to the specifications in Hütte, vol. 1, 26th edition, p. 401, figure 97. This profile form was determined by Birnbaum (reference 11) on the basis of a lift distribution which can be conveniently represented by a formula. If Γ is the circulation about the profile and $k = \partial\Gamma/\partial x$ is the circulation per unit length, the distribution of the circulation over the vane chord t is

$$k = \frac{\Gamma}{t \sin\left(\alpha + \beta - \frac{1}{2}\gamma\right)} \left[\sin\alpha \frac{2}{\pi}\sqrt{\frac{1 - 2\,x/t}{1 + 2\,x/t}} + \sin\beta \frac{4}{\pi}\sqrt{1 - \left(\frac{2\,x}{t}\right)^2} - \sin\gamma \frac{2}{\pi}\sqrt{1 - \left(\frac{2\,x}{t}\right)^2} \right]$$

in which

$$\beta = 1/4\ (\psi + \varphi), \qquad \gamma = 1/4\ (\psi + \varphi)$$

(fig. 7). The theoretical lift is then

$$c_a = 2\pi \sin\left(\alpha + \beta - \tfrac{1}{2}\gamma\right)$$

---

*On this high c_a value is based, however, the marked displacement of the vortex c.g. which materially affects the result, as already mentioned.

and the moment coefficient is

$$c_m = \frac{\pi}{2} \sin (\alpha + 2\beta - 5/4\gamma)$$

The theoretical, infinitely thin profiles have the advantage that no velocity changes due to the altered cross section need to be considered. One was chosen with the notations of figure 7,

$$\psi = 12^\circ \qquad \varphi = 6^\circ$$

We then obtain, for $c_a = 1.35$, an angle of attack $\alpha = 8^\circ\ 40'$ and a moment coefficient $c_m = 0.428$. The center of pressure lies at $x_m = 0.317\ t$.

Figure 8 shows the basic profile, thus plotted, at $8^\circ\ 40'$ angle of attack with superposed square-mesh system and below it the mesh system of the grid flow in the region of the omitted vortex. If it is observed that the center of pressure of the profile must coincide with the center of the omitted vortex, the transformation automatically follows with the aid of the mesh system and yields the basic profile with an angle of attack of $64^\circ\ 45'$ to the direction of the flow.

3. Behavior of the Profile of First Approximation

The test results (section III) show that a profile was found which very well satisfies the specified conditions of good distribution of the velocity and static pressure in the emerging jet and involves minimum losses. Since, however, in order to obtain this result, still another change of 8.25 degrees is necessary, the agreement between the theory and test results must be considered entirely unsatisfactory. Hence our next task is to discover the cause of these discrepancies. For this purpose we will compare the measured circulation distribution with the theoretical.

The theoretical circulation distribution is known, since the equation for the profile form was calculated by Birnbaum from a suitable assumption for the lift distribution. For the individual vane in rectilinear planar flow the lift is

$$A = \rho w \int_0^t \frac{d\Gamma}{dx} d x$$

or

$$A = \rho w \int_0^t k d x$$

if we again introduce

$$\frac{d \Gamma}{d x} = k$$

Figure 20 represents the circulation distribution in non-dimensional form as k/w. The abscissa x, which, theoretically, is to be taken along the projection in the inflow direction, is here taken approximately along the development of the profile. The theoretical distribution of the circulation along the development of the grid profile is then easily determined from the formula

$$\Gamma = \int_0^t k d x = \int_0^T K d X$$

X, in this case, also being taken along the profile. We then have

$$d \Gamma = k d x = K d X$$

or

$$K = k \frac{d x}{d X} \quad \text{and} \quad \frac{K}{w} = \frac{k}{w} \frac{d x}{d X}$$

Instead of an analytical transformation function, we use, just as in the transformation of the profile, the square-mesh system, taken directly from the distortion scale dx/dX for all points.

The measured circulation distribution is derived in simple manner from the pressure distribution. If p_d' and p_s' denote the pressures on the pressure and suction

sides of an individual vane, then, for an element of the individual vane calculated along the vane profile in parallel planar flow with w as the velocity in infinity,

$$d A = (p_d' - p_s') d x = \rho w d \Gamma$$

and

$$\frac{d \Gamma}{d x} = k = \frac{p_d' - p_s'}{\rho w} \quad \text{and} \quad \frac{k}{w} = \frac{p_d' - p_s'}{\rho w^2}$$

Correspondingly, if $d P_y$ denotes the force acting on an element $d X$ of the vane profile in the grid direction, v the velocity normal to the grid direction, θ the angle between the profile element and the direction of v, and p_d and p_s the respective pressures on the pressure and suction sides, we have at the vane in the grid

$$d P_y = (p_d - p_s) d X \cos \theta = \rho v d \Gamma$$

and

$$\frac{d \Gamma}{d X} = K = \frac{p_d - p_s}{\rho v} \cos \theta \quad \text{and} \quad \frac{K}{w} = \frac{p_d - p_s}{\rho v w} \cos \theta$$

We must remember that the velocity component v normal to the grid is not constant. It is derived from the field of flow (in the region of the missing vortex) for each point of the contour.

From the comparison of the circulation distribution measured at the grid vane with the theoretical (fig. 23) it appears that the circulation is considerably more concentrated in the middle of the profile, while too little lift is generated in the forward portion of the profile. The after portion works approximately in the desired manner.

These discrepancies are obviously due to the fact that, in the sharply curved flow on the forward portion of the vane, there is a strong pressure increase on which is superposed the pressure increase on the suction side of the normal vane which is installed in this flow. There is thus produced a pressure increase of such magnitude that the boundary layer is detached. On the leading edge

of the guide vane vortices are now produced which modify the pressure distribution until the pressure increase becomes normal.

This change in the pressure distribution causes a rearward shift of the center of gravity of the vortex. Moreover, with the sharp curvature of the vane profile, the center of gravity of the vortex layer can no longer remain on the contour, as we could assume in the first approximation for the basic profile.

For our theoretical calculation, it was only assumed that the concentrated vortices substituted for the vane lie in the circulation c.g. of the vane. Hence, if this c.g. is shifted, the vane must also be shifted, so that the c.g. of the circulation distribution will be restored to its correct location.

In figure 8 the dash line represents the profile as shifted by the amount of the travel of the c.g. The displacement must be effected by transferring the circulation c.g. (designated by Z in figure 8), as found on the vane profile, to the basic profile with the aid of the square-mesh system; letting this point Z coincide with the center of the omitted vortex in the grid field of flow (Z' identical with 0); and repeating the diagram with the aid of the mesh system.

We thus obtain a profile with an angle of attack of 59 degrees in the inflow direction, which is quite accurately congruent with the original profile of first approximation. The difference in the angle of attack is only about 2° 30' as compared with the correctly measured angle.

4. The Profile of Second Approximation

In deducing the profile of first approximation, it was assumed that, for calculating the field of flow in which the profile is installed, the vane with its circulation can be considered as concentrated in a point. Now the curvature of the streamlines determines the curvature of the profile. It could therefore be assumed that the concentration of the vortex in a point is too inaccurate. Hence a second approximation was made for the vane form, in which a distribution of the circulation corresponding

to the actual relations (here appropriately the distribution found in the first approximation) was taken as the basis.

The field of flow was again calculated according to the above-mentioned Betz method, only with the difference that the interference velocities u and v for every point of the field first had to be obtained from an integration of the elementary flows, each of which was derived from the elementary circulation $d\Gamma$ of a vane (fig. 9). The field of flow, as thus calculated, is represented in the region of the missing vortex in figure 10 as a square-mesh system. In this system the profile of second approximation is plotted with consideration of the location of the vortex c.g. as determined for the profile of first approximation. In figure 10 the vortex c.g. is assumed to be located on the contour. It is of no importance in this case, since the actual shifting into the interior of the region included in the profile has already been allowed for in the plotting of the field of flow by the location of the elementary circulations. We thus obtain a 56-degree angle of attack with the direction of inflow, while the experiments showed that the most favorable angle of attack for this profile was 55 degrees.

On comparing the practically obtained circulation distributions for the profiles of first and second approximation (fig. 23), we find that no appreciably better approximation of the circulation distribution to the theoretically desired was not attained. Both profiles behaved almost the same. The error due to the concentration of the vortices is of no practical significance even for very pronounced vortices.

As regards low resistance and uniform velocity distribution behind the guide vanes the profiles of the first and second approximations may be regarded as practically equivalent, the profile of first approximation having only a very slight aerodynamic superiority.

III. THE EXPERIMENTS

1. Investigation of a Deflection Angle with Profiles of First Approximation Developed According to Section II in a Square Tunnel.

In judging a deflection corner with installations, we must distinguish the influence of the installations from the influence of the cross-sectional shape. With a square or rectangular cross section, we can, at least for the middle section (parallel to the plane of the bend) calculate for an approximately two-dimensional flow, which had to be assumed in the theoretical treatment. A square section of 200 by 200 millimeters was therefore chosen.

The arrangement shown in figure 11 served for the investigation of the corner in a square tunnel. Guide vanes and several narrow-meshed pieces of wire gauze in the conduit from the fan to the test space insured uniform distribution of the velocity over the cross section (fig. 12). The portion of the tunnel before the bend was made very short, in order to reduce the development of the boundary layers as much as possible. With a length of about 1.5 times the width of the tunnel, another test point for the pressure p_2 could be added.

At the test point for the pressure p_2, a strong brass plate had to be set into the tunnel wall, since the orifice in the original thin zinc wall did not prove sufficiently reliable and the slight local deflections of the wall affected the pressure indications considerably. At the corner a straight piece with a length equal to twice the width of the tunnel was added before the full blast was used.

The vanes were mounted in a removable frame which enabled their easy exchange and adjustment without taking the whole apparatus apart and also greatly facilitated the control of the accuracy of the work.

The mean velocity $\overline{w}$ in the experimental tunnel was about 28 m/s, and the Reynolds Number was about 4×10^4. The velocity $\overline{w}$ was determined from the pressures p_1 and p_2 (kg/m^2) according to the formula

$$\overline{w} = \sqrt{\frac{\lambda(p_1 - p_2)}{\frac{1}{2}\rho}}$$

The value of λ was found, from measuring the velocities in the cross section before the bend, to be 1.00*.

*On the basis of the cross-sectional relations and the Bernoulli equation, the velocity in the center of the cross section would be $\lambda = 1.07$. Due, however, to the retardation along the walls, the mean velocity was somewhat smaller (fig. 12), namely 1.00, as given above.

The velocity distribution behind the bend was determined in the outlet cross section. There it could be assumed that the static pressure was constant throughout the cross section, so that the velocity measurements may be considered very reliable. The static pressure was also measured in a plane 20 mm behind the trailing edges of the guide vanes. For this purpose the measuring instrument had to be placed at 45 degrees to the tunnel wall. After various experiments the static-pressure indicator shown in figure 13 was found to be the most suitable.

In the investigation of the corner with profiles of first approximation (fig. 14), it was immediately evident that the first-calculated angle of attack of 64° 45' was too large. It was therefore gradually reduced to 56° 30' as the most favorable angle. As shown in figure 15, a variation between 56 and 58 degrees does not have much effect on the velocity distribution, but probably does on the distribution of the static pressure behind the vanes and on the pressure loss.

Figures 16 and 17 show the respective velocity distributions behind a 90-degree elbow and behind a 90-degree bend without guide vanes. Comparison with figure 15 very clearly shows the advantage of the guide vanes.

At this point I will call attention to some fundamental principles regarding the determination of the pressure and of the lost energy. In practical hydraulics it is customary for the calculation of the energy losses in fluid conduits to employ the resistance coefficient ζ of the individual members (tube cross section, bends, etc.). This coefficient ζ indicates that the passage of a certain amount of gas or liquid through any part of the conduit requires a certain pressure difference Δp equal to ζ times the dynamic pressure q of the mean velocity $\overline{w}$ in the entrance cross section. $q = \frac{1}{2} \rho \overline{w}^2$ and $\overline{w} = Q/F$, where Q is the quantity of fluid passing through per unit of time (m^3/sec) and F is the entrance cross section. Hence,

$$\zeta = \frac{\Delta p}{\frac{1}{2} \rho \overline{w}^2}$$

According to what precedes, this formula for the pressure-loss coefficient is based on the unidimensional viewpoint, i.e., as if the velocity were uniformly distributed over the cross section. In a bend the different fluid particles

generally undergo very different energy losses, so that it may be necessary to allow for these differences in the determination of the energy consumption.

The total energy content per unit volume is the total pressure $p + \frac{1}{2} \rho w^2$, where p is the static pressure and $\frac{1}{2} \rho w^2$ is the dynamic pressure. The elementary outputs are the quantities of energy per second flowing past the individual points. They are represented by the formula

$$(p + \tfrac{1}{2} \rho w^2) w \, d F$$

in which the unit is (mkg/sec). The total energy loss, as based on the momentum before the corner, is

$$\kappa = \frac{[\int(p+\frac{1}{2}\rho w^2) w dF] \text{ before bend} - [\int(p+\frac{1}{2}\rho w^2) w dF] \text{ after bend}}{[\int(\frac{1}{2}\rho w^3 dF)] \text{ before bend}}$$

It is seen that, with w and p assumed to be constant throughout the cross section, the equation passes into the expression for ζ.

The coefficient of loss κ is important, when it is desired to allow for energy transformations which affect the nature of the flow. For the deflection angles tested in this investigation, it is only necessary to use the loss coefficient ζ, since the deflection does not appreciably affect the nature of the flow.

For the most favorable angle of attack of 56° 30', the coefficient of resistance was $\zeta = 0.134$. This high value is due, however, to the insufficient length of approach for eliminating the strong initial disturbances of the flow. For the calculation of the resistance of conduits with built-in elbows, this value seldom comes in question.

2. Pressure-Distribution Measurements at the Exit Profile and at the Profile of First Approximation. Total Pressure Distribution in the Vortex Trail.

a) Pressure-Distribution Measurements.- For judging the behavior of the profiles, it was necessary to compare the actual circulation distributions with the theoretical.

The actual circulation distribution was determined, as already described, from the pressures measured on the surface of the profile.

It seemed desirable at first to verify experimentally the circulation distribution of the basic profile (individual vane in parallel rectilinear flow). Since however, it was to be expected from the outset that, for an individual vane, such a high value of c_a (1.35) as was adopted for the design of the guide vane, due to the separation phenomena on the suction side, could no longer be attained (at least not with the theoretical angle of attack), the comparison between the theoretical circulation distribution and that determined experimentally with the help of pressure-distribution measurements was made with a theoretical $c_a = 1.00$. In order to measure the surface pressure at the exit profile, a double-walled model of the profile was made. The chord t was 175 mm; the span, 250 mm; and the thickness, about 3 mm (figs. 18 and 19). The middle section was provided with test holes of 0.5 mm diameter, which were connected with brass tubes. From these brass tubes, rubber tubes led to the tubes of a multiple manometer. The readings were made by photographing the manometer tubes together with the accompanying scale. Terminal disks of 310 mm diameter were attached to the ends of the vane, in order to obtain a smooth flow. Figure 18 shows the suspension of the vane in the wind tunnel, the nearer terminal disk having been removed in order to show the vane. The angle of attack was regulated by turning the bars on the outer sides of the disks about their pivots.

In figure 20 the upper curve represents the theoretical circulation distribution for $c_a = 1.35$; the middle curve, the theoretical distribution for $c_a = 1.00$; and the bottom curve, the theoretical distribution for $c_a = 1.00$ and the angle of attack $\alpha = 5^\circ 30'$.

The comparison of the theoretical with the measured circulation distribution shows that the character of the two curves is much the same, excepting that the c_a value found by planimetry is only about 65 percent of the theoretical. This observation that the integration of the pressures along the surface of the vane yields a considerably lower lift than the theoretical, agrees with the earlier observation by Betz (reference 12). This is chiefly due to the surface friction. An enlargement of the end disks would only lessen the induced drag, but have no appreciable effect on the magnitude of the lift in the middle

section. That here only about 65 percent of the theoretical lift was obtained (instead of 75 to 80 percent, which can ordinarily be assumed) is probably due in part to the fact that a plate-like profile, such as used here, offers more resistance than the customary wing profile.

For the grid flow, despite this discrepancy, we must at first calculate with the theoretical lift distribution. Due to the different nature of the pressure increases, etc., the behavior of the boundary layers will be quite different. Our task is therefore to study these effects. Due to the pressure drop in the vicinity of the trailing edge of the vane, it is probable that, where we have the maximum deviations from the theoretical values for the isolated vane, we obtain only a small error for the assembled vane. The following comparison of the total-pressure measurements behind the trailing edge of the isolated vane and of the assembled vane, will show how much less the disturbance due to friction (separation) is in the grid.

A special model according to figure 21 was made for measuring the pressure distribution on the guide vanes, since the dimensions of the wind-tunnel model were too small for this purpose. It consisted of five vanes, which were mounted between top and bottom plates at intervals of 85 mm and could be rotated. The grid model corresponded exactly in scale to the model of the individual vane. The middle vane was made hollow and was provided, in its middle section, with a series of 0.5 mm holes. The diameter of the air jet directed against the vanes was 300 mm, and the distance between the top and bottom plates, required to produce a smooth flow, was 250 mm. The direction of the deflected air flow was read on an angle scale with the aid of three silk threads at three different heights.

Figure 22 shows the pressure distribution on the surface of the grid profile of first approximation for three angles of attack. The 90-degree deflection was effected for $\alpha = 56^{\circ}\ 30'$ in absolute agreement with the measurement in the closed tunnel, i.e., the deflection was produced entirely by the guide vanes without the assistance of the walls. The circulation distribution (fig. 23), as calculated from the pressure distribution, and the conclusions deduced will be given in section II, 3.

b) Total-pressure distribution in the vortex trail.- The loss of energy in the air stream after passing the

profile is a criterion for the losses through friction (separation). It is therefore possible to determine the frictional losses by determining the total pressure in a cross section of the vortex trail (reference 13). The investigation of the vortex trail was undertaken with the models used for determining the circulation distribution, since the vanes in the closed tunnel were too small for this purpose.

The measuring plane, both for the individual vane and for the grid as a whole, was 15 mm behind the trailing edges. The results are plotted nondimensionally in figure 24. The total energy loss from surface friction and separation is represented by the area between the line corresponding to the total pressure before the vane $\left(\frac{p_{tot}}{\frac{1}{2}\rho w} = 1\right)$ and the curve for the total pressure behind the vane.

The total pressure behind the individual vane was measured at 5° 30' angle of attack, the same angle at which the pressure-distribution measurements were made, so that the circulation about the isolated vane corresponding to $c_{a\ theor.} = 1.00$ in the ratio 6.60/8.88 was smaller than the circulation about the assembled vane. It is recognized that, despite the smaller circulation, the loss of energy from profile resistance is greater for the isolated vane than for the assembled vane. Hence even here we find our original assumption confirmed that the vane in the grid can withstand a relatively heavy load without producing unfavorable resistance conditions.

The loss through friction and separation on the vanes, as determined by planimetry of the loss areas, is only about 5 percent of the momentum, while the pressure loss measured in the closed tunnel is 13 to 14 percent. The principal losses do not therefore depend on the lift-drag ratio of the vane profile, so that no appreciable reduction of the losses can be expected from a further improvement of the profile.

3. Experimental Investigation of the Profile of Second Approximation

The experimental investigation of this profile (fig.

25) corresponded exactly to that of the profile of first approximation. The theoretical investigation yielded an angle of attack of 56° for the profile of second approximation with consideration of the travel of the circulation c.g. produced by the high c_a in conjunction with the sharp curvature and confirmed in the first approximation. The most favorable distribution of static pressure and velocity throughout the cross section behind the vanes, with simultaneous minimum pressure loss, was obtained at an angle of attack of 55° (fig. 26). The coefficient of resistance is 0.138, i.e., somewhat larger than for the profile of first approximation (0.134). The course of the pressure-distribution curve, which is less uniform on the suction side of the profile of second approximation (fig. 27) than for the first approximation, likewise indicates a certain superiority of the profile of first approximation. In like manner the result of the total-pressure measurement in the vortex trail shows a somewhat greater resistance (fig. 24).

4. Experiments with Other Deflection Angles and Groups of Deflection Angles*

a) Experiments with other deflection angles**.- In addition to deflection angles of 90 degrees, tests were also made at angles of 60, 45, and 30 degrees (figs. 28-30), the profiles being made according to the first approximation. For the deflection of 60 degrees, the calculation was made with $c_a = 1.35$, while, for deflections of 45 and 30 degrees the profiles were based on $c_a = 1.00$, since otherwise the vanes would not have been close enough.

The velocity and pressure distributions are represented in figures 31-33. For losses and angles of attack, see table in section IV. It is noteworthy that, at 30 and 40 degrees deflection, no change from the theoretical angle of

---

*The experiments of this section were performed by Dr. Flachsbart, to whom I am greatly indebted for the use of the experimental results.

**The experiments in this section were tried at the suggestion and under the direction of Dr. Flachsbart, to whom I am greatly indebted for the privilege of using the results.

attack is required. This means that, at the larger angles of attack, the marked discrepancies are attributable, at least in part, to the high c_a. On the other hand, the curvature of the streamlines is here considerably less, so that a shifting of the profile along the streamlines does not affect the angle of attack so much.

b) Experiments with groups of deflection angles.- The state of flow is known to be affected for a long distance by a normal bend or elbow in the adjoining conduit. If, e.g., a second bend is introduced into the conducting system before the disturbance has died out, this second bend will have a different coefficient of loss from the first, which has an undisturbed inflow*.

The better the deflection in our sense is, i.e., the less the nature of the flow is changed, just so much less the mutual influence will be. In the ideal case the coefficients of loss, even at short distances between the individual angles, must simply be added.

The following group arrangements

$2 \times 90^\circ$ $2 \times 45^\circ$ $3 \times 60^\circ$

were investigated with the profile arrangement calculated according to the first approximation (figs. 34-36). The loss coefficients (see table), in all three arrangements, are smaller than the sum of the loss coefficients of the corresponding individual angles. This result is accidental, as shown by subsequent control tests at the individual angles of a group. The above-found energy losses for individual angles are not absolute minima, but can be reduced in certain cases by particularly careful finishing of the guide vanes in the workshop. In the groups there were some angles which caused somewhat less energy loss than the previously tested individual angles.

5. Ninety-Degree Deflection in Tunnel with Circular Cross Section

The difference in the behavior of deflections of different cross-sectional shapes depends on the different de-

*In this connection, numerous tests have already been made by Weisbach (reference 14).

velopment of the secondary currents (reference 15). The latter consist essentially of double vortices produced by the friction, with their axes in the direction of flow. Their unfavorable effect on the pressure loss in bends is due to the fact that they converge the boundary-layer material, especially that retarded by friction, on the inner wall of the bend, where there is already a tendency toward separation, thus greatly promoting separation and the formation of vortices.

If it is now possible, through suitable devices (guide vanes or the like) to restrict the separation on the inner wall, as likewise the formation of the secondary flow, to the rear part of the bend, the effect of the cross-sectional shape on the resistance will disappear.

The profile of first approximation was selected for the installation in the bend of the tunnel of circular cross section, because it showed the least resistance of any of the profiles tested. The test fully confirmed the above considerations (fig. 37) and yielded exactly the same result as for the installation in the square tunnel, namely the angle of attack of 56° 30', and almost the same loss coefficient (0.136 instead of 0.134). The cross-sectional shape does not affect the behavior of the deflection with favorable profiles.

6. Taking Flow Pictures

The arrangement shown in figure 38 served for obtaining photographs of the flow through the grid. A channel of 200 mm width was set in a water tank about 200 mm deep. The guide vanes were those of first approximation, the angle of attack being 56° 30'. The second bend in the channel (on the right-hand side of the picture) did not serve for observations, but was necessary for conducting the water smoothly through the channel.

The direction of the flow was rendered visible by means of fine aluminum powder sprinkled on the surface of the water, which had to be colored red to prevent reflection of light from the bottom of the channel. Figure 39 is a picture with the complete row of guide vanes, while in figure 40 one of the vanes in the middle had been removed, in order to create conditions similar to those on

which the calculation was based. Pictures thus obtained cannot be expected to furnish a perfectly accurate basis for checking the calculation. The omission of one vane changes the circulation about the neighboring vanes, though the theory requires all vortices to be of equal strength. The neighboring vanes should therefore have been shifted so as to restore the original circulation. The developing of marked vortex formations on the backs of the neighboring inner vanes, however, made this impossible from the outset.

During the experiment it was observed that, with the great density of the powder required for the large area to be photographed and by the corresponding distance from the camera, the scattered particles, despite all precautionary measures such as paraffining the walls and the vanes, showed so great a tendency to accumulate on one side or the other of the channel that sometimes the streamlines on the surface differed noticeably from the deeper flow as recognized by direct observation of the added coloring matter. Therefore the pictures give only a relatively rough idea of the actual conditions, but are nevertheless very instructive. The narrowness of the wake and of the vortex trail behind the vanes is particularly noticeable.

IV. SUMMARY AND CONCLUSIONS

The results of the investigation may be summed up as follows. By taking as the basis profiles with high c_a, such as have proved practically favorable, it was not possible to find a satisfactory form of grid simply on the assumption that the flow is potential. The requirements called for the most uniform possible velocity distribution behind the bend and the smallest possible losses. In order to meet them, it was necessary to take friction and its effects into account. The pressure increments in the flow, modified with respect to the conditions for a simple airplane wing, change the separation phenomena with the chosen high c_a, so that the center of pressure travels rearward. By taking this into account, a satisfactory agreement is obtained between the theoretical consideration and the experimental results. It may be assumed, with the choice of a more suitable exit profile, which (with the center of pressure farther rearward at the outset) yields a more favorable pressure distribution on the forward part of the

grid, that better agreement will be obtained between potential theory and reality. At low c_a (30 and 45 degrees deflection) we obtain, according to the potential theory, results which require no further correction.

The state of the jet leaving the grid differs so little from that before the bend that several deflections may occur closely behind one another, without their behavior being materially influenced.

As a further result of the fact that the nature of the jet is not changed in passing through the grid (i.e., that no appreciable separation from the inner wall of the bend nor formation of secondary vortices occurs), it was found that the cross-sectional shape of the channel (excepting extreme forms) has no perceptible effect on its behavior.

The table contains a summary of the vane forms tested. From it the calculated and the experimental angles of attack and the loss coefficients can be taken. Furthermore the loss coefficients, which were obtained without the installation of vanes, are included.

In figures 14, 25, 28, 29, and 30 the forms of angles tested are represented with the installations in their final position. Figure 41 shows the profiles of first approximation with their principal dimensions, based on the distance between the vanes, for the various angles of attack.

What improvements with respect to the energy loss are to be effected by the installation of guide vanes, are shown by the graphical comparison of the loss coefficients. from the most important energy measurements in bends and elbows with the loss coefficients found for various deflection angles after the installation of suitably shaped guide vanes (fig. 42). In addition to the recent measurement by Kirchbach (ref. 16), the previous measurement by Weisbach (ref. 17) is included, since the Weisbach values are still commonly used in practice. The resistance coefficients for elbows with square cross section were obtained from the same models, which served for the investigation of the deflection angles with vane grids. They were included for the sake of completeness, although, due to the short outlet, they could make no claim to general applicability.

For bends in cylindrical tubes, we have plotted a series of measurements by Hofmann (reference 18), which

includes bends of various bending ratios R/d and various degrees of roughness but only one deflection angle (90 degrees), and also a series of measurements by Bouchayer (reference 19) with only one bending ratio, but various deflection angles. Bouchayer's experiments were made with power-plant pipes, which were quite rough but probably corresponded well with normal conditions.

If it is desired to keep the energy loss as small as possible, guide vanes can be advantageously installed in elbows down to about 30 degrees deflection angle, when the elbow cannot be replaced by a bend of adequate radius. If a velocity distribution of greatest possible uniformity behind the deflection is desired, the installation of a vane grid may be justified for even smaller deflection angles.

A uniform velocity distribution in the inflow is assumed for small energy loss in deflections with the aid of guide vanes in every case according to direction and magnitude.

Translation by Dwight M. Miner,
National Advisory Committee
for Aeronautics.

REFERENCES

1. Prandtl, L.: Ergebnisse der Aerodynamischen Versuchsanstalt, Göttingen, Report I, p. 17, third edition, Munich, 1925.

2. Lell, J.: Beitrag zur Kenntnis der Sekundärströmung in gekrümmten Kanälen. Diss. Darmstadt, 1913.

3. Wirt, L.: New data for the design of elbows in duct systems. Gen. electr. Rev. 30, 1927, p. 286.

4. Kirsten, H.: Experimentelle Untersuchung der Entwicklung der Geschwindigkeitsverteilung der turbulenten Rohrströmung. Dissertation, Leipzig, 1927.

5. Saph, A. V. and Shoder, E. W.: Trans. Amer. Soc. Civil Engr. 47, 1908, p. 183.

Gregory, W. B. and Shoder, E. W.,: Trans. Amer. Soc. Mech. Engr. 30, 1908, p. 351; also reference 2.

6. Weisbach, J.: Experimentalhydraulik, p. 148, Freiburg, 1855.

Bouchayer, A.: Los pertes des charges dans les conduits condes et embranchements. Hydro-electr. Kongress Grenoble, 1925, Engineering, 1925, II, p. 241.

Nippert, H.: Über den Strömungsverlust in gekrümmten Kanälen. Forsch.-Arb. Ing.-Wes. No. 320, 1929. (With numerous references).

Hofmann, A.: Der Energieverlust in 90°-Rohrkrümmern mit gleichbleibendem Kreisquerschnitt. Mitt. hydrodyn. Inst. Techn. Hochschule Munich, No. 3, 1929.

Kirchbach, H.: Der Energieverlust in Kniestücken. Mitt. hydrodyn. Inst. Techn. Hochschule Munich, No. 3, 1929.

Bambach, R.: Plötzliche Umlenkung (Stoss) von Wasser in geschlossenen, unter Druck durchströmten Kanälen. Forsch.-Arb. Ing.-Wes., No. 327, 1930.

Christiani, K.: Experimentelle Untersuchung eines Tragflügels bei Gitteranordnung. Luftf. Forsch. 2, No. 4, 1928.

7. Schilhansl, M.: Z.F.M., vol. 19, 1928, p. 151.

8. Spannhake, W.: Eine strömungstechnische Aufgabe der Kreiselradforschung und ein Ansatz zu ihrer Lösung. Mitteilung des Instituts für Strömungsmaschinen der Technischen Hochschule Karlsruhe, No. 1, p. 4. Munich and Berlin, 1930.

Spannhake, W. and Barth, W.: Z. f. a. M. M., 19, 1929, p. 466.

9. Betz, A.: Tragflügel und hydraulische Maschinen. Handbuch der Physik, vol. VII, p. 238, Berlin, 1927.

10. Betz, A.: Ing.-Arch. 2, 1931, p. 359.

11. Birnbaum, W.: Z. f. a. M. M., 3, 1923, p. 290.

12. Betz, A.: Untersuchung einer Joukowskyschen Tragfläche. Mitt. Aerodyn. Versuchsanstalt, zu Göttingen. First edition. Reprint, Leipzig, 1930.

13. Betz, A.: A Method for the Direct Determination of Wing-Section Drag. T.M. No. 337, N.A.C.A., 1925.

14. Weisbach, J: Experimentalhydraulik. Freiburg, 1855.

15. Lell, J.: Beitrag zur Kenntnis der Sekundar-Strömung in gekrümmten Kanälen. Diss. Darmstadt, 1913.

Nippert, H.: Über den Strömungsverlust in gekrümmten Kanälen. Forsch.-Arb. Ing.-Wes., No. 320, 1929.

16. Kirchbach, H.: Die Energieverluste in Kniestücken. Mitt. Hydr. Inst. Tech. Hochschule Munich, No. 3, 1929.

17. Weisbach, J: Experimentalhydraulik, p. 148. Freiberg, 1855.

18. Hofmann, A.: Der Verlust im 90°-Rohrkrümmer mit gleichbleibendem Kreisquerschnitt. Diss. Techn. Hochschule, Munich, 1929.

19. Bouchayer, A.: Les pertes des charges dans les conduits condes et embrachements. Hydro-electr. Kongress, Grenoble, 1925, Engineering II, 1925, p. 241.

TABLE

Angle of deflection	Shape of cross section	Form of grid	Angle of attack		Coefficient of resistance	
			theoretical	experimental	with guide vanes	without vanes
90°	Square	Profile of 1st approximation	64° 15'* and 59°	56° 30'	0.134	1.63**
90°	Square	Profile of 2nd approximation	56°	55°	0.138	1.63
90°	Circular	Profile of 1st approximation	59°	56° 30'	0.136	1.0
60°	Square	Profile of 1st approximation	43°*	38°	0.146	1.08
45°	Square	Profile of 1st approximation	33° 15'*	33° 15'	0.142	0.53
30°	Square	Profile of 1st approximation	22° 30'*	22° 30'	0.100	0.15
2 x 90°	Square	Profile of 1st approximation	59°	56° 30'	0.260	
2 x 45°	Square	Profile of 1st approximation	33° 15'*	33° 15'	0.266	
3 x 60°	Square	Profile of 1st approximation	43°*	38°	0.304	
90° bend $\frac{R}{b} = 0.7$	Square	Partitions	-	-	0.24	1.10

*Calculated without taking into account the displacement of the circulation c.g.
**Too high, due to the inadequate length of the outlet channel.

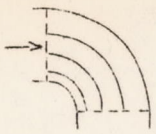

Figure 1.-Bend with partitions.

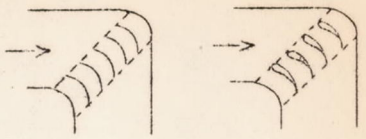

Figures 2a,2b.-Deflection by guide vanes.

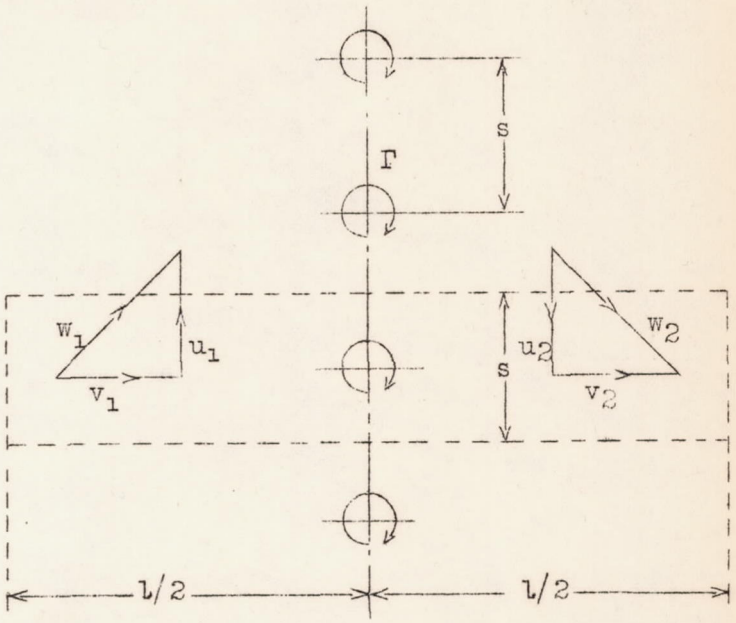

Figure 3.-Vortex series with parallel flow.

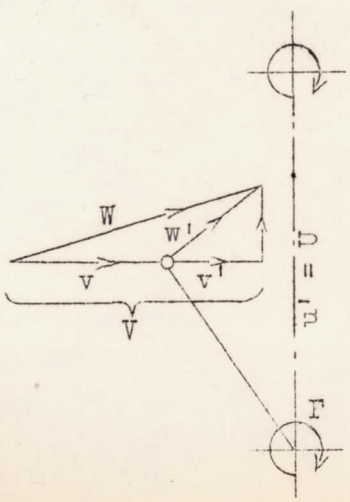

Figure 4.-Velocity components near votices.

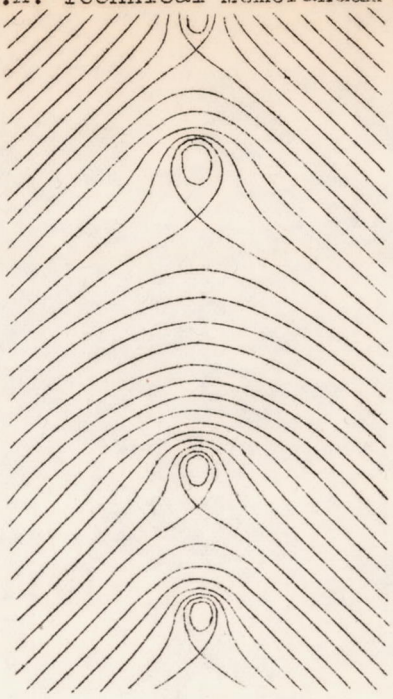

Figure 5.-Field of flow of vortex series(one vortex omitted).

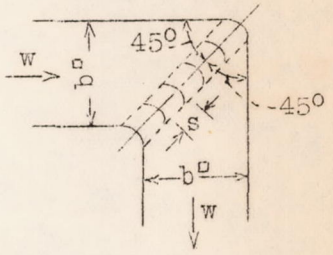

Figure 6.-Ninety-degree deflection with guide vanes.

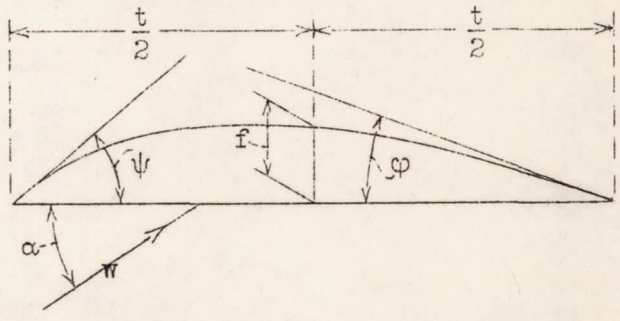

Figure 7.-Birnbaum's profile with variable curvature.

1. Theoretical center of pressure of basic profile,0.

2.Point in field of basic profile corresponding to position of vortex c.g. on guide vane, Z.

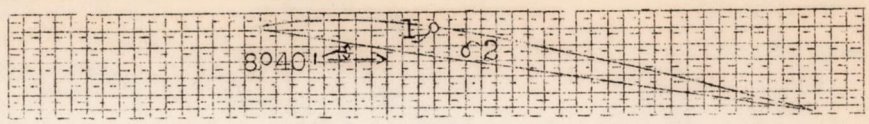

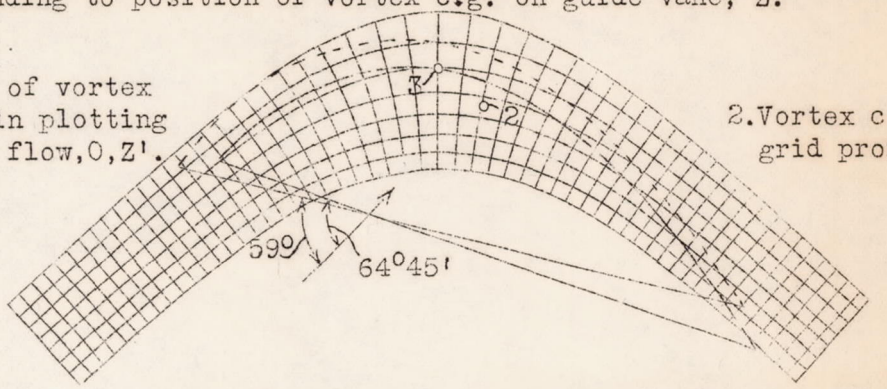

Figure 8.-Basic profile and construction of profile of first approximation.

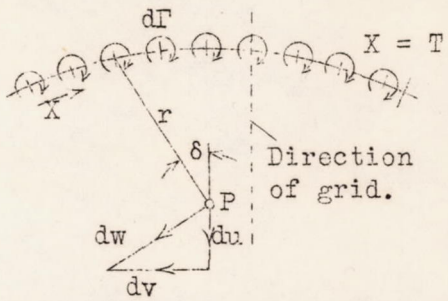

Figure 9.-Distribution of circulation over chord of guide vane.

1.Point in field of basic profile corresponding to position of vortex c.g. on grid profile.

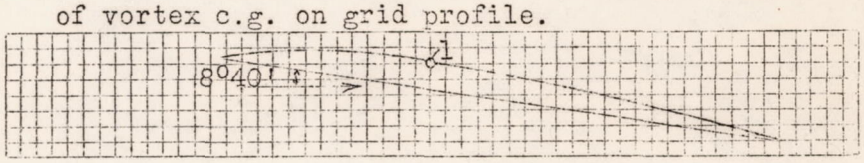

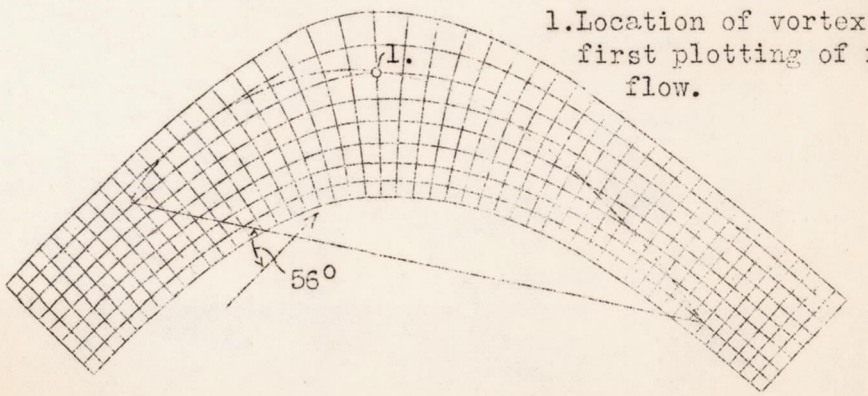

Figure 10.-Construction of profile of second approximation.

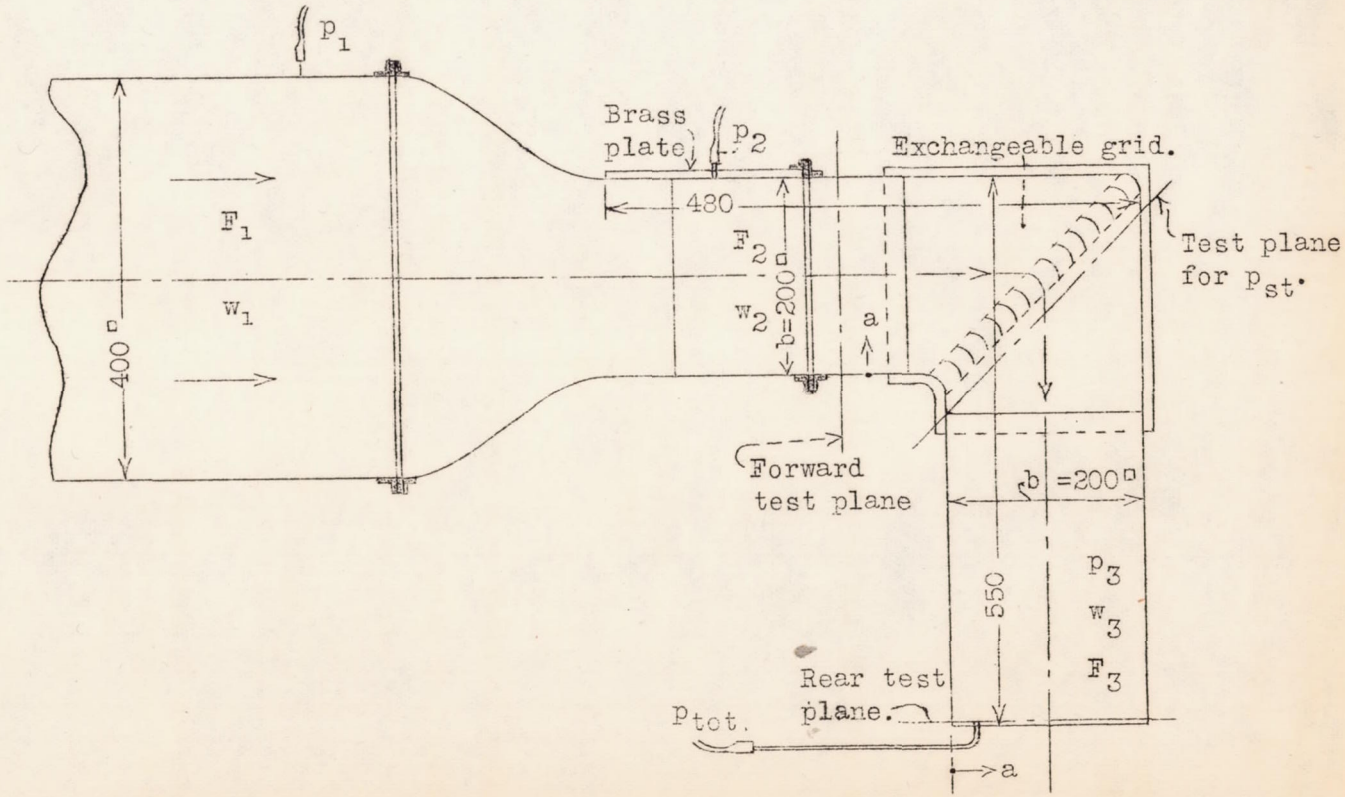

Figure 11.-Apparatus for measuring distribution of velocity and static pressure.

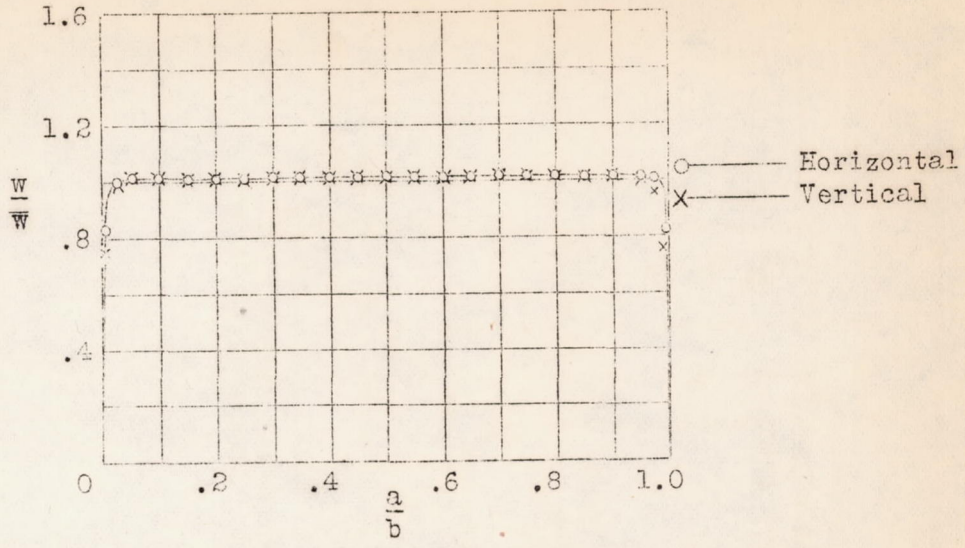

Figure 12.-Velocity distribution before deflection.

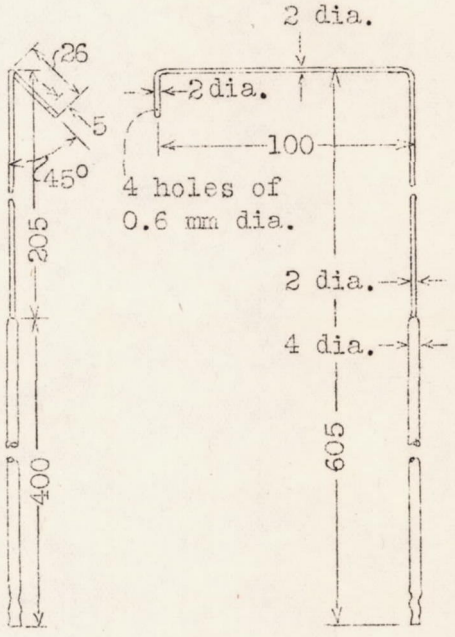

Figure 13.-Device for measuring static pressure close behind grid.

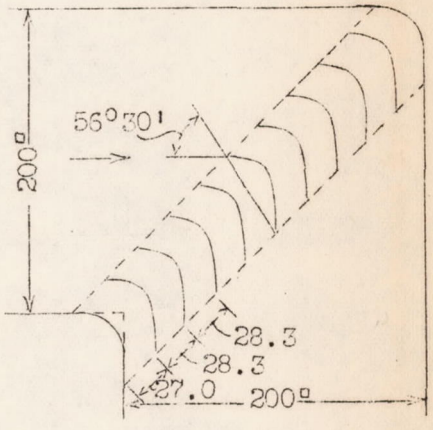

Figure 14.-90° deflection, profile of first approximation.

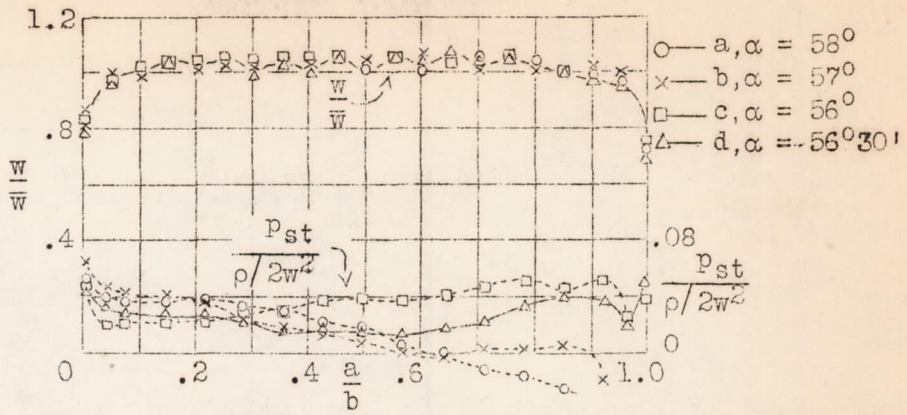

Figure 15. 90° deflection, profiles of first approximation. Velocity and pressure distribution.

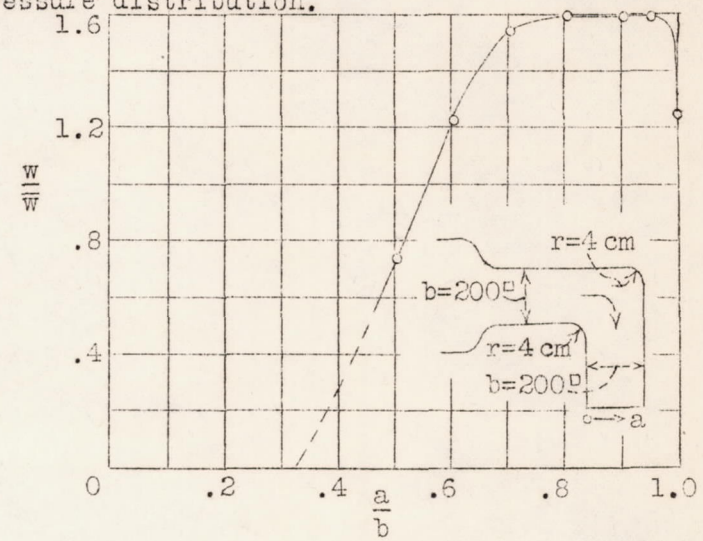

Figure 16. 90° deflection(elbow)without guide vanes.Vel. distribution.

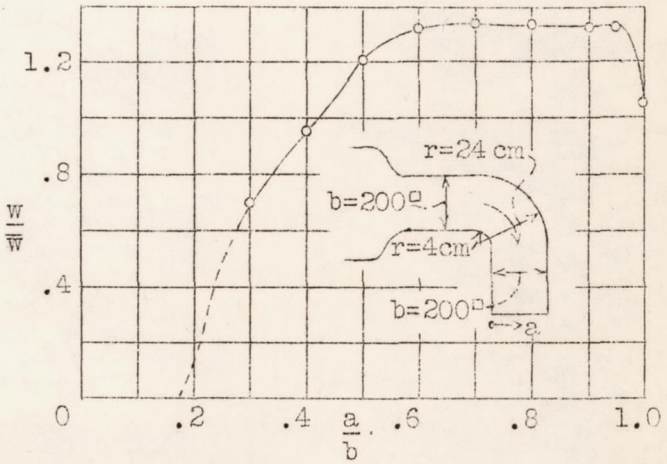

Figure 17. 90° deflection(bend)without guide vanes.Vel.distribution.

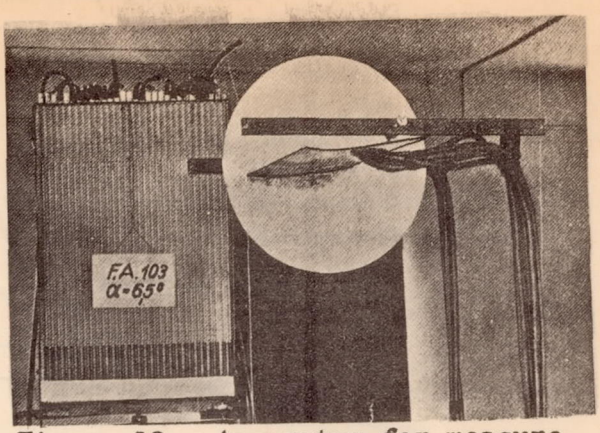

Figure 18.- Apparatus for measureing pressure distribution on basic profile (nearer disk removed).

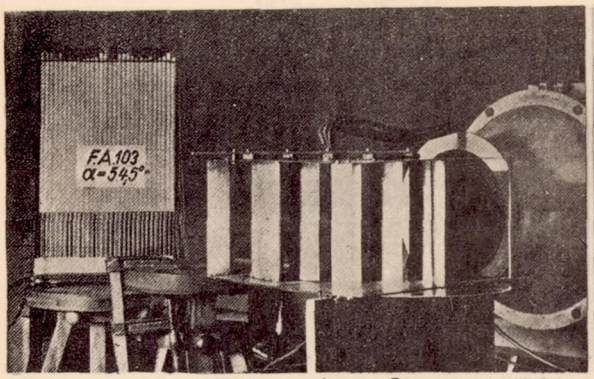

Figure 21.- Apparatus for measureing pressure distribution on gird profile.

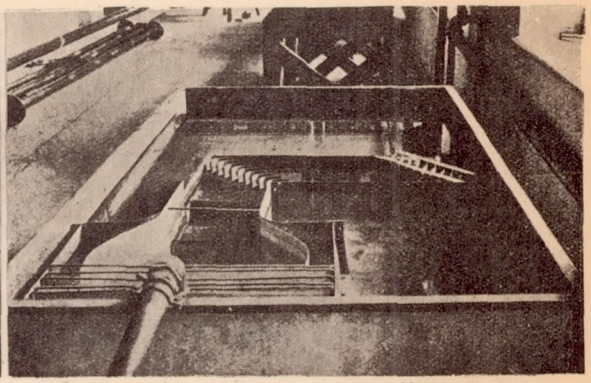

Figure 38.- Apparatus for taking flow pictures.

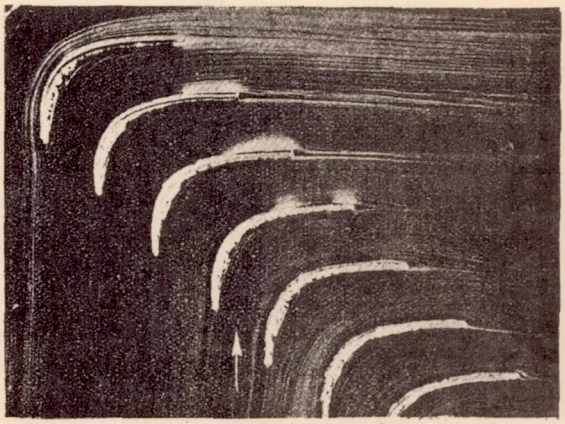

Figure 39.- Flow through gird. Profiles of first approximation.

Figure 40.- Flow through gird; one vane removed.

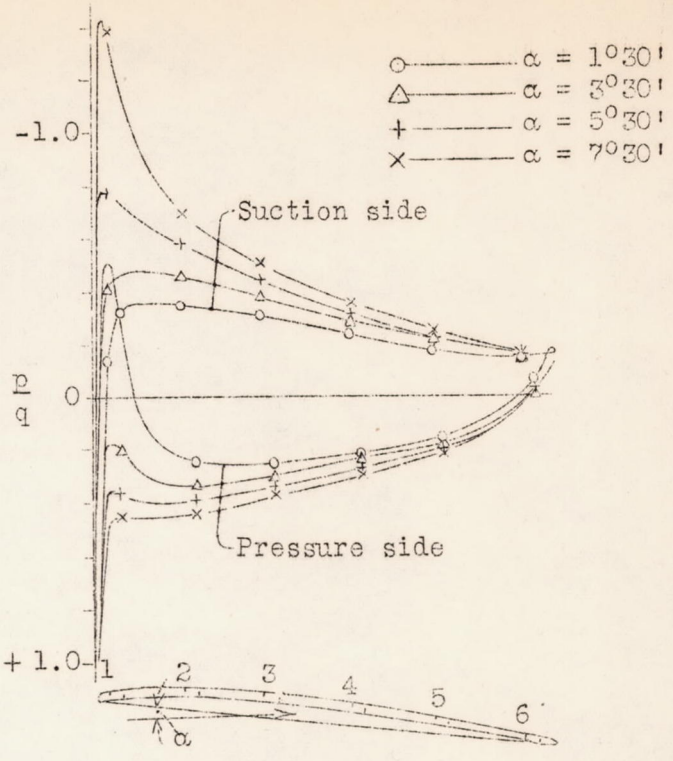

Figure 19.-Basic profile. Pressure distribution.

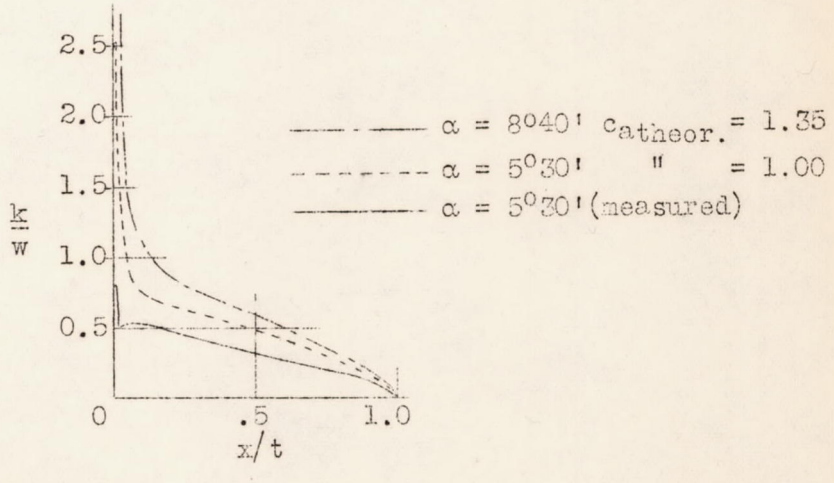

Figure 20.-Basic profile. Circulation distribution.

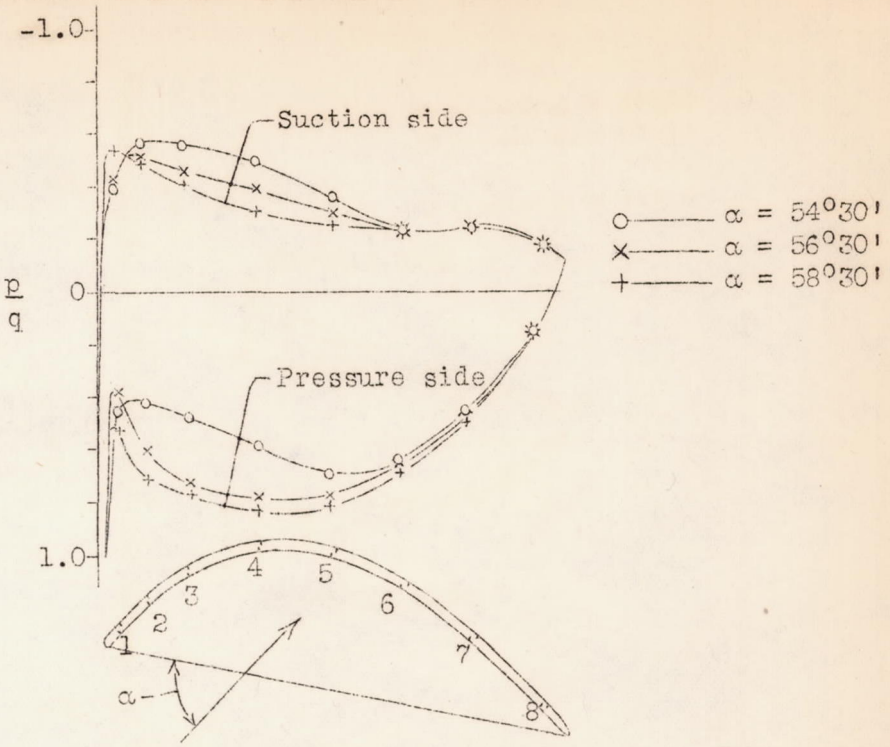

Figure 22.-Profile of first approximation. Pressure distribution.

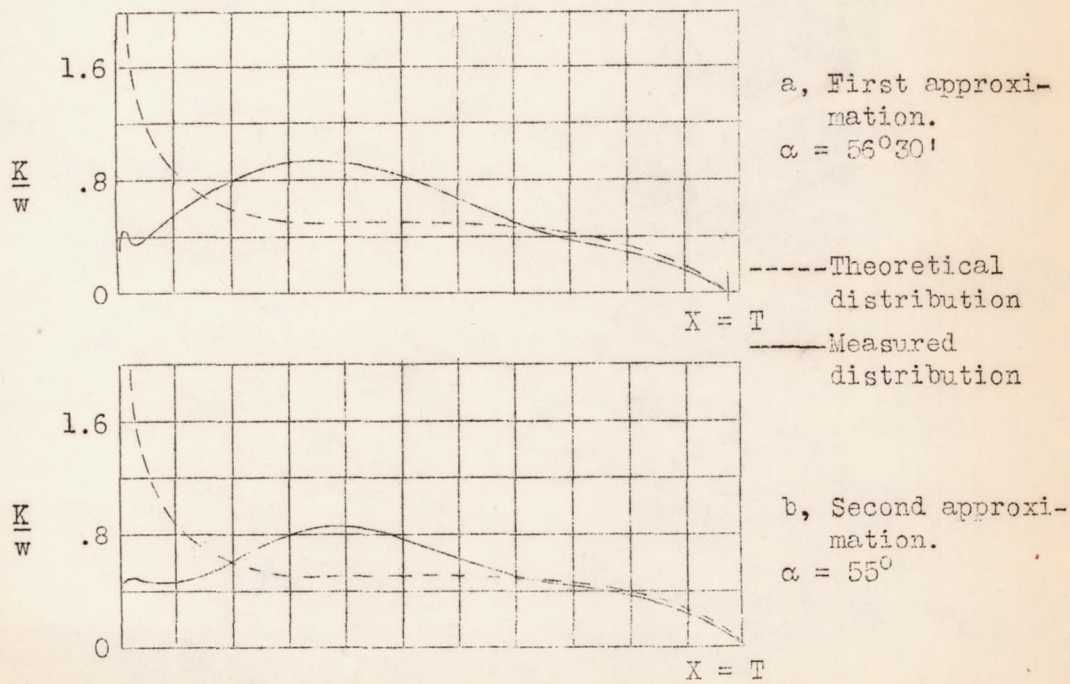

Figures 23a, 23b-Circulation distribution of profiles.

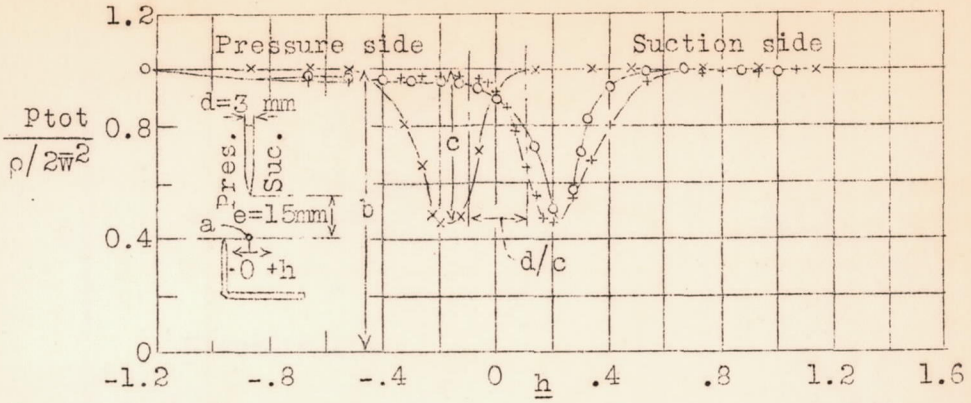

a,Plane of total-pressure measurement.
b,Energy of undisturbed flow = 1.0
c,Frictional loss

×—— Individual vane Γ/ws=6.60
○—— Vane in grid Γ/ws=8.88, profile of 1st approx.
+—— Vane in grid Γ/ws=8.88, profile of 2nd approx.

Figure 24.-Total pressure distribution in vortex trail.

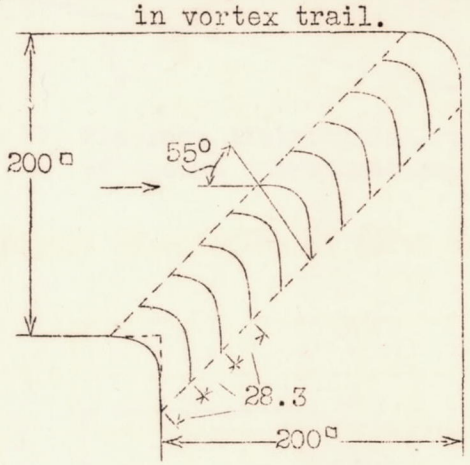

Figure 25. 90° deflection. Profiles of second approximation.

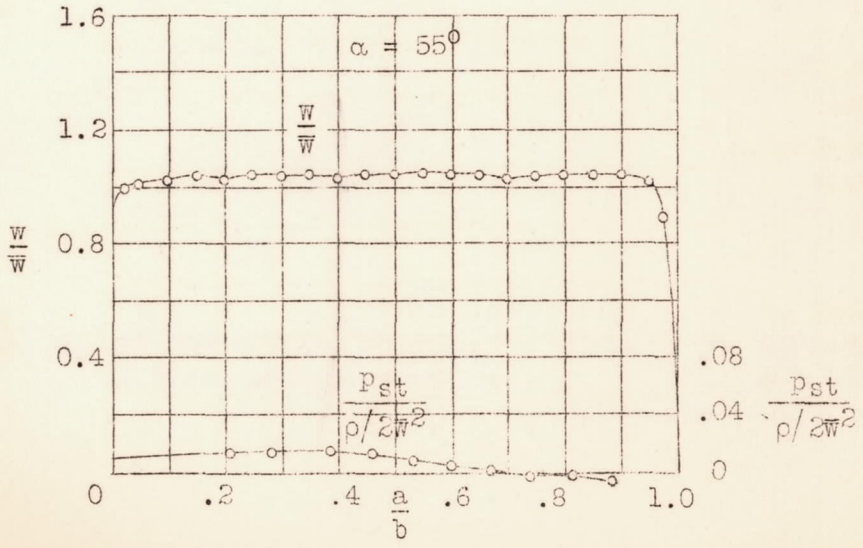

Figure 26. 90° deflection. Profiles of second approximation. Velocity and pressure distribution.

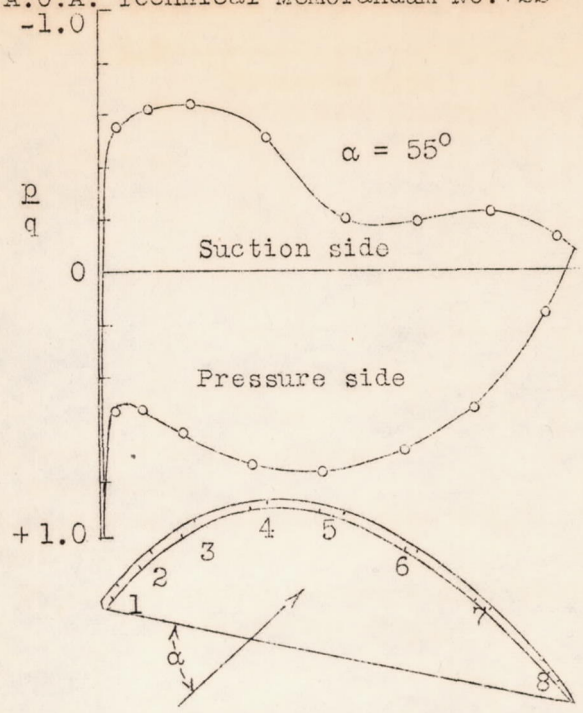

Figure 27. Pressure distribution. Profile of second approximation.

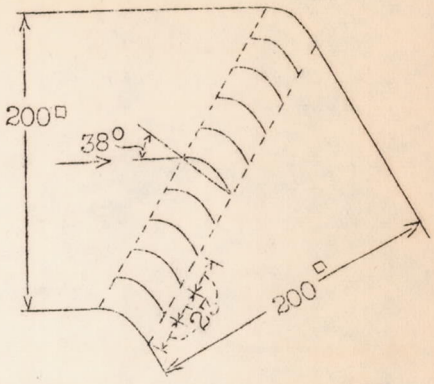

Figure 28. 60° deflection. Profiles of first approximation.

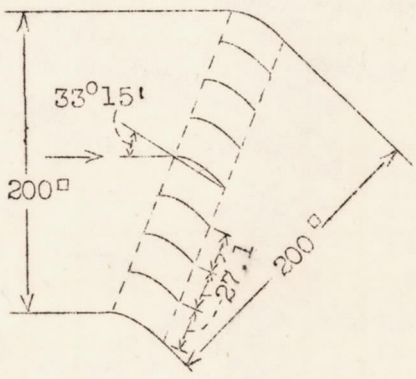

Figure 29. 45° deflection. Profiles of first approximation.

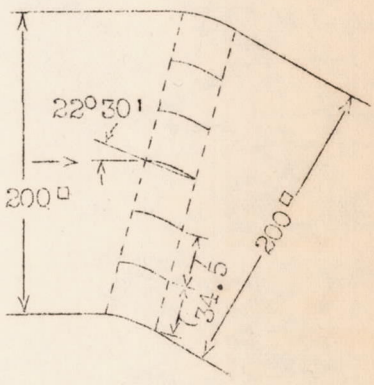

Figure 30. 30° deflection. Profiles of first approximation.

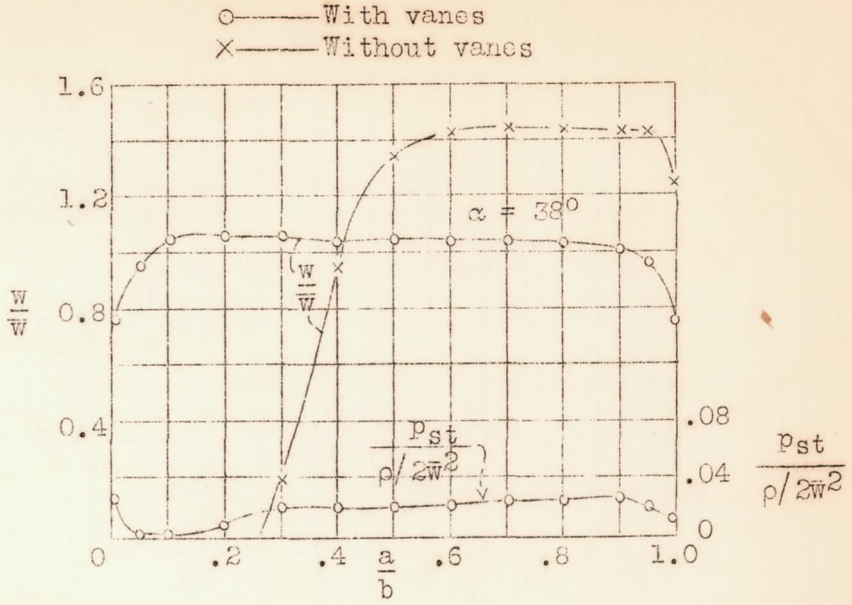

Figure 31. 60° deflection. Profiles of first approximation. Velocity and pressure distribution.

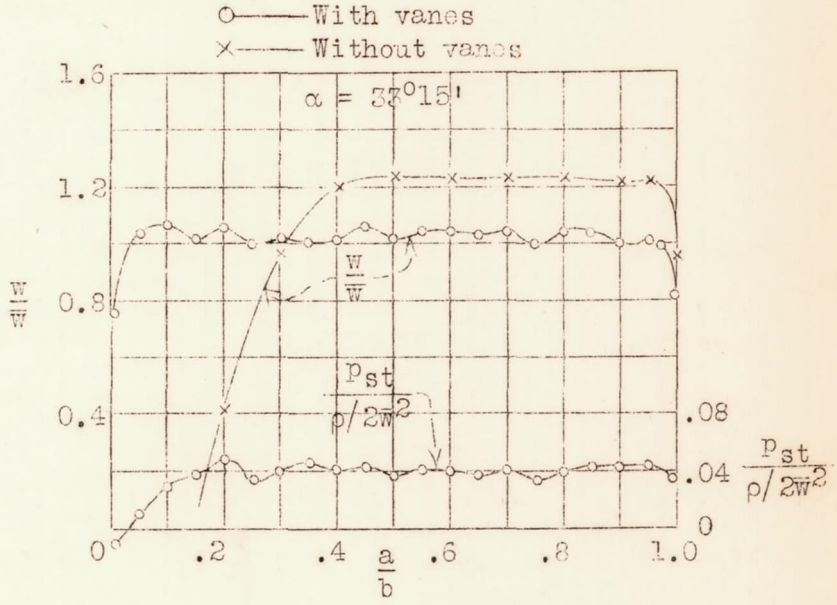

Figure 32. 45° deflection. Profiles of first approximation. Velocity and pressure distribution.

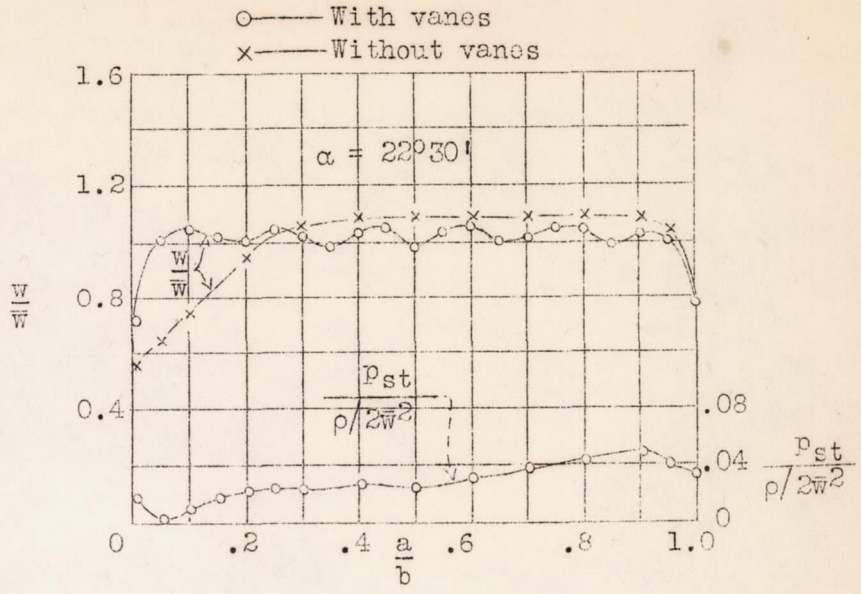

Figure 33. 30° deflection. Profiles of first approximation. Velocity and pressure distribution.

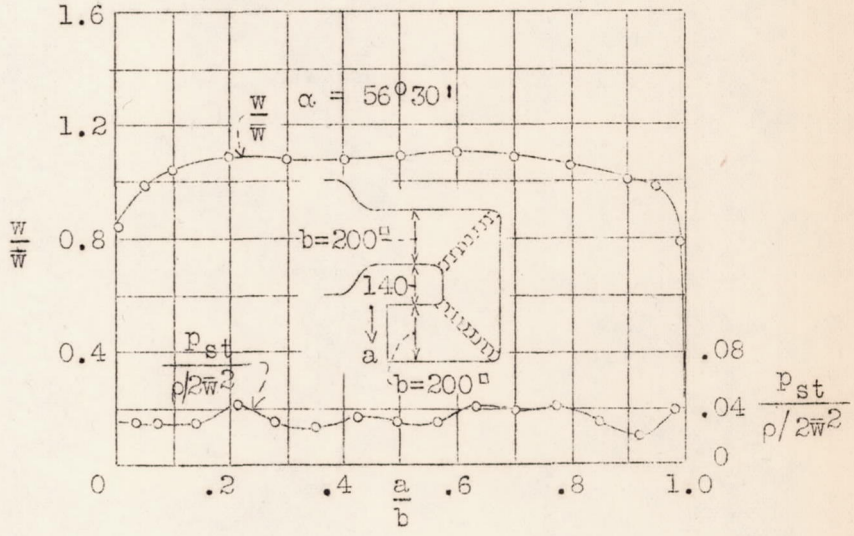

Figure 34. 2 x 90° deflection. Profiles of first approximation. Velocity and pressure distribution.

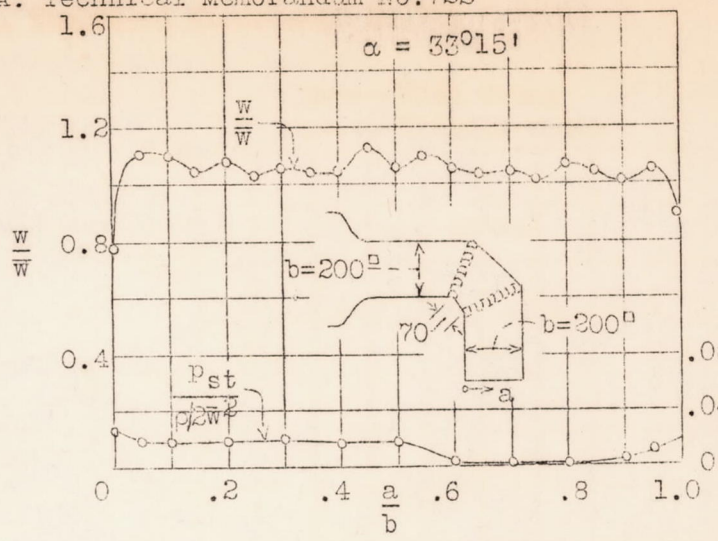

Figure 35. 2 x 45° deflection. Profiles of first approximation. Velocity and pressure distribution.

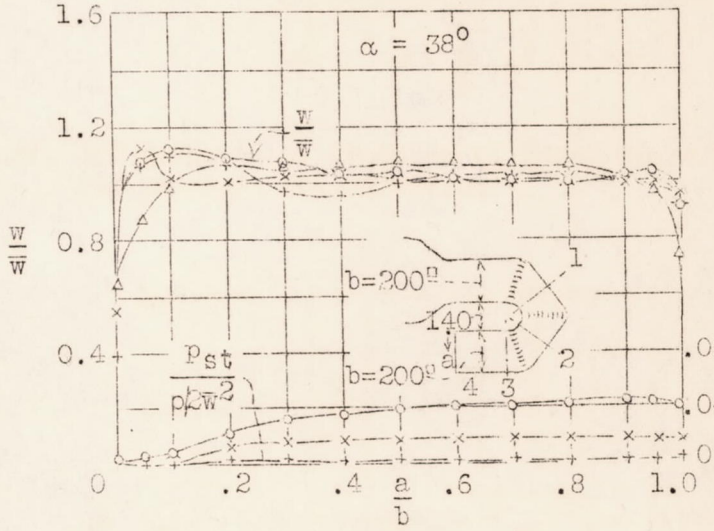

Figure 36. 3 x 60° deflection. Profiles of first approximation. Velocity and pressure distribution.

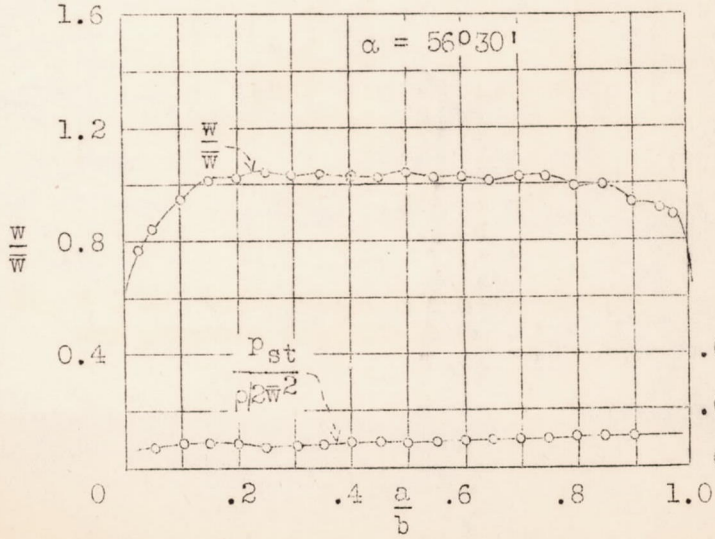

Figure 37. 90° deflection. Profiles of first approximation. Circular cross section. Velocity and pressure distribution.

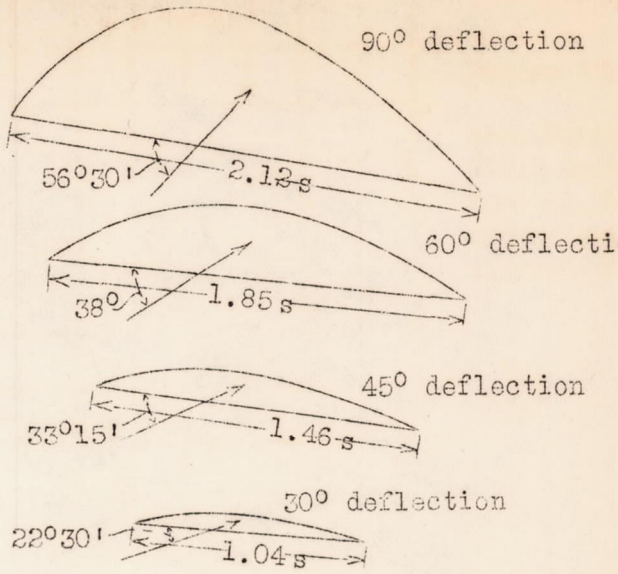

s = distance between vanes in direction of grid.

Figure 41.-Profiles of first approximation for grids with different angles of deflection.

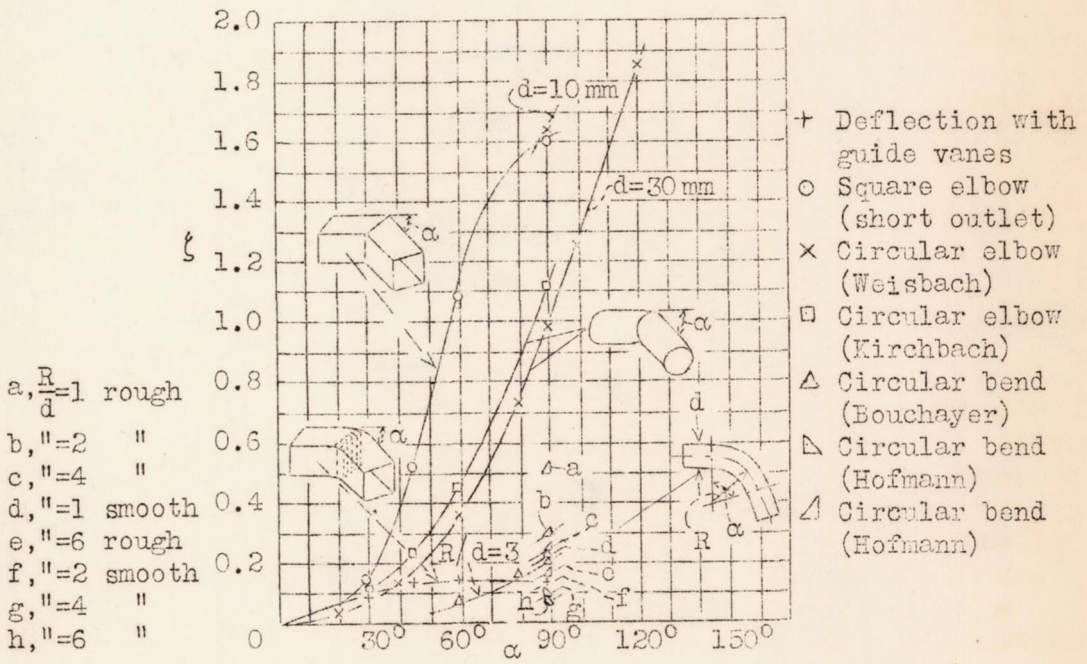

Figure 42.-Resistance of various deflections.